THE ASTROPHYSICAL JOURNAL, 457:490–499, 1996 February 1

A GROUP OF GALAXIES AT REDSHIFT 2.38[1]

PAUL J. FRANCIS,[2,3] BRUCE E. WOODGATE,[4,3] STEPHEN J. WARREN,[5] PALLE MØLLER,[6] MARGARET MAZZOLINI,[2]
ANDREW J. BUNKER,[7] JAMES D. LOWENTHAL,[8,9] TED B. WILLIAMS,[10] TAKEO MINEZAKI,[11]
YUKIYASU KOBAYASHI,[12] AND YUZURU YOSHII[13,14]

Received 1995 June 2; accepted 1995 August 8

ABSTRACT

We report the discovery of a group of galaxies at redshift 2.38. We imaged ~10% of a claimed supercluster of QSO absorption lines at $z = 2.38$. In this small field (2′ radius), we detect two Lyα-emitting galaxies. The discovery of two such galaxies in our tiny field supports Francis & Hewett's interpretation of the absorption-line supercluster as a high-redshift Great Wall.

One of the Lyα galaxies lies 22″ from a background QSO and may be associated with a multicomponent Lyα absorption complex seen in the QSO spectrum. This galaxy has an extended (~50 kpc), lumpy Lyα morphology surrounding a compact, IR-bright nucleus. The nucleus shows a pronounced break in its optical-UV colors at ~4000 Å (rest frame), consistent with a stellar population of mass $\sim 7 \times 10^{11}\ M_{\odot}$, an age of greater than 500 Myr, and little ongoing star formation. C IV emission is detected, which suggests that a concealed active galactic nucleus is present. The Lyα emission is redshifted by ~490 km s^{-1} with respect to the C IV emission, probably because of absorption. Extended Hα emission is also detected; the ratio of Lyα flux to Hα is abnormally low (~0.7), probable evidence for extended dust.

This galaxy is surrounded by a number of very red ($B - K > 5$ mag) objects, some of which have colors that suggest that they too are at $z = 2.38$. We hypothesize that this galaxy, its neighbors, and a surrounding lumpy gas cloud may be a giant elliptical galaxy in the process of bottom-up formation.

Subject headings: galaxies: clusters: individual (2139−4434) — galaxies: distances and redshifts

1. INTRODUCTION

The extent of galaxy clustering at high redshifts ($z > 1$) is controversial. Cold dark matter (CDM) and similar models predict that most large-scale structure forms at redshifts below 1. This is consistent with the rapid evolution in galaxy clusters seen between $z \sim 0.5$ and the present (Butcher & Oemler 1978; Edge et al. 1990). Further evidence comes from the apparently weak clustering of faint blue galaxies at $z \sim 0.7$ (Efstathiou et al. 1991) and the weak clustering of Lyα forest clouds (see, e.g., Carswell & Rees 1987).

On the other hand, an increasing body of data suggests that galaxies at redshifts above 1 are strongly clustered on large scales. Evidence comes from metal-line QSO absorption systems (see, e.g., Heisler, Hogan, & White 1989; Jakobsen & Perryman 1992; Foltz et al. 1993; Møller 1995; Williger et al. 1995), from the association of Lyα-emitting galaxies with damped Lyα absorption systems and QSOs (Wolfe 1993; Djorgovski et al. 1985), and from the often serendipitous discovery of individual clusters (e.g., Dressler et al. 1993; and, possibly, Giavalisco, Steidel, & Szalay 1994).

Francis & Hewett (1993) claimed to have discovered two coherent structures of gas, at least 10 comoving Mpc in size, one at redshift 2.38, the other at 2.85. These postulated structures cause Lyα absorption at matching redshifts in the spectra of two background QSOs separated by 8′. These authors discussed two possibilities: either the gas structures are primordial pancakes or Great Wall–style superclusters. In both cases, these structures would be the most dramatic examples yet of large-scale structure at high redshift.

In this paper, we attempt to confirm the existence of one of Francis & Hewett's enormous structures. We have studied a small part of the postulated $z = 2.38$ structure using a wide range of optical, IR, and radio observations on 10 different southern-hemisphere telescopes (see § 2). Our initial aim was to search for Lyα-emitting sources at this redshift using narrow-band Fabry-Perot imaging. We found at least two Lyα-emitting galaxies at $z = 2.38$ (see § 3.1), one of which has a remarkable extended Lyα morphology. Extensive follow-up observations at many frequencies revealed a number of other possible galaxies at $z = 2.38$.

[1] Based on observations collected at Cerro Tololo Inter-American Observatory, the European Southern Observatory (La Silla, Chile), Siding Spring Observatory, the Australia Telescope, and the Anglo-Australian Observatory.

[2] School of Physics, University of Melbourne, Parkville, Victoria 3052, Australia; pjf, marg@physics.unimelb.edu.au.

[3] Visiting Astronomer, Cerro Tololo Inter-American Observatory. CTIO is operated by the Association of Universities for Research in Astronomy, Inc. (AURA), under contract to the National Science Foundation.

[4] NASA Goddard Space Flight Center, Code 681, Greenbelt, MD 20771; woodgate@uit.dnet.nasa.gov.

[5] Astrophysics Group, Imperial College, Blackett Laboratory, Prince Consort Road, London SW7 2BZ, UK; s.j.warren@ic.ac.uk.

[6] Space Telescope Science Institute, Baltimore, MD 21218, on assignment from the Space Science Department of ESA; moller@stsci.edu.

[7] Department of Physics, University of Oxford, Keble Road, Oxford OX1 3RH, UK; a.bunker1@physics.oxford.ac.uk.

[8] Lick Observatory, Santa Cruz, CA 95064; james@lick.ucsc.edu.

[9] Hubble Fellow.

[10] Physics and Astronomy Department, Rutgers University, P.O. Box 849, Piscataway, NJ 08855-0849; williams@fenway.rutgers.edu.

[11] Department of Astronomy, Faculty of Science, University of Tokyo, Bunkyo-ku, Tokyo 113, Japan; umineza@c1.mtk.nao.ac.jp.

[12] National Astronomical Observatory, Mitaka, Tokyo 181, Japan; yuki@merope.mtk.nao.ac.jp.

[13] Institute of Astronomy, University of Tokyo, Mitaka, Tokyo 181, Japan; yoshii@omega.mtk.ioa.s.u-tokyo.ac.jp.

[14] Research Center for the Early Universe, School of Science, Bunkyo-ku, Tokyo 113, Japan.

We describe our observations in § 2; results are shown in § 3 and discussed in § 4. Throughout this paper, we assume that $H_0 = 75\,\mathrm{km\,s^{-1}\,Mpc^{-1}}$ and $q_0 = 0.5$.

2. OBSERVATIONS

Because of limited observing time and poor weather, we were able to observe only a small part of one of Francis & Hewett's postulated structures. We chose to study the $z = 2.38$ structure and imaged the field around one of the two background QSOs, 2139−4434. The absorption-line system in 2139−4434 at $z = 2.38$ consists of at least three components, a central one of wavelength 4108.5 Å and neutral hydrogen column density $\sim 7 \times 10^{18}$ cm^{-2} and two lower column density systems (see Fig. 1). Given the limited resolution of our spectra, we have not attempted a decomposition of the two subsidiary absorption systems, but we estimate their wavelengths as being 4101 and 4119 Å. All three may well be blends of lower column density lines.

2.1. *Optical Imaging*

The first step in our imaging campaign was to search for redshifted Lyα emission from galaxies at $z = 2.38$. A field surrounding the QSO 2139−4434 was imaged on the nights of 1994 June 4 and 5, by use of the Rutgers Fabry-Perot system (Gebhardt et al. 1994) with Goddard etalons, on the CTIO 4 m telescope. The etalon was set to a central wavelength of 4110 Å with a width of 30 Å. The relatively large width was chosen to allow for possible peculiar velocities relative to the main absorption system, as suggested by the wavelengths of the subsidiary absorption systems. We alternated 1800 s exposures on-band with 360 s exposures off-band. Off-band exposures were also taken through the etalon, but with the plate spacing altered to shift the central wavelength away from the absorption-line wavelength and with the order-blocking filter removed. This increased the count rate from continuum sources by a factor of ~ 5. The similarity of the setup between on- and off-band exposures was intended to prevent any ghost images' showing up as narrowband excess objects. The telescope was offset by $\sim 5''$ in a random direction between pairs of on- and off-band exposures to improve flat-fielding and as an additional precaution against ghosts.

Six pairs of on- and off-band images were taken on each night (Fig. 2). Seeing was $\sim 1''.6$ (FWHM) throughout. Images taken on the first night suffered from poor throughput in the order-blocking filter; a more efficient filter was used on the second night. A narrowband flux limit of 8.4×10^{-17} ergs cm^{-2} s^{-1} for a point source was reached (3 σ). All images were reduced with standard IRAF[15] procedures, then shifted and added using inverse-variance weighting to maximize the final signal-to-noise ratio. Because of light cirrus during the observations, only relative photometry was obtained, bootstrapped from CCD-calibrated UK Schmidt plate scans. This introduces an uncertainty of ~ 0.15 mag in the photometry.

Candidate narrowband excess objects were selected in a variety of ways. On- and off-band images were blinked and compared by eye, and both aperture photometry and DAOPHOT were used. All approaches were cross-checked and found to yield consistent answers. Automatic procedures needed substantial human intervention because of the strong signal-to-noise gradient across the frames that was caused by the shifting and adding, which principally manifested itself in spurious sources near the edge of the field. All fluxes quoted in this paper are total fluxes. For fainter unresolved objects, photometry was carried out with a small aperture (diameter $\sim 1''.6$, the seeing FWHM) and corrected up to a total flux by use of the point-spread function (PSF) of bright, isolated stars in the field. Flux and magnitude limits are quoted for the area around QSO 2139−4434 where the noise is a minimum, for an aperture of diameter $\sim 1''.6$.

An additional *B*-band image was obtained on the CTIO 0.9 m telescope with the Tek 2k chip, which yielded a $12' \times 12'$ field centered on a point midway between the two background QSOs that included the fields around both QSOs. A total of 10,800 s exposure was obtained on the night of 1994 June 7.

I- and *B*-band images of the field around 2139−4434 were obtained on the night of 1994 August 5 with the EFOSC camera (see Eckert, Hofstadt, & Melnick 1989) on the ESO 3.6 m telescope. Exposure times were 2700 s in *B* and 1620 s in *I*, and the seeing was poor ($\sim 2''.5$). The *I*-band image reached a limiting magnitude of 23 (3 σ). A weighted sum of the two *B*-band images reached a limiting magnitude of 24.7 (3 σ). Photometry of these frames was carried out as described above.

Astrometry for all frames was bootstrapped from positions in the COSMOS database, maintained on-line at the Anglo-Australian Observatory. In each image, five stars were used to obtain a six-coefficient plate solution. Residuals from the fit (rms) in each coordinate were $0''.15$ for the CTIO 4 m images, $0''.12$ for the ESO 3.6 m images, and $0''.12$ for the Siding Spring 2.3 m IR images.

2.2. *IR Imaging*

IR imaging was obtained on the nights of 1994 September 25–28 on the Siding Spring Observatory's 2.3 m telescope with the PICNIC near-IR camera (see Kobayashi et al. 1994). The detector's field of view was centered midway between the QSO and galaxy B1 (see § 3.1). PICNIC has a 256 × 256 near-IR camera and multiobject spectrometer (NICMOS) chip, with $0''.5$ pixels. Two hundred fifty exposures, each of 17 s, were obtained in both *H* and *K'* bands, in $1''.0$ seeing. Limiting magnitudes were 21.0 in both *H* and *K'* (3 σ). Seventy-five exposures, each of 67 s, were taken through an interference filter of

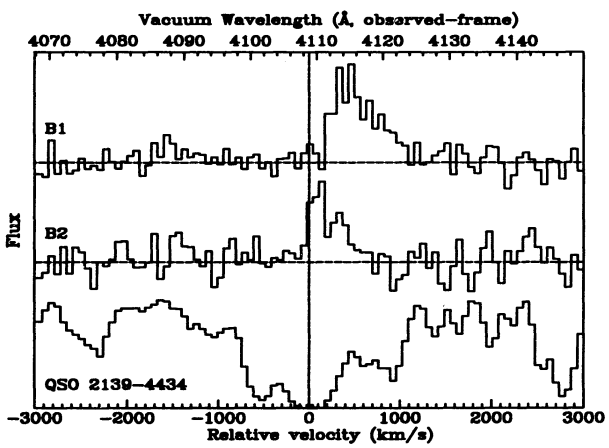

FIG. 1.—NTT spectra of B1 and B2 and the QSO 2139−4434, showing the Lyα lines. A higher resolution spectrum of this QSO can be found in Francis & Hewett (1993).

[15] IRAF is distributed by the National Optical Astronomy Observatories, which are operated by AURA under cooperative agreement with the National Science Foundation.

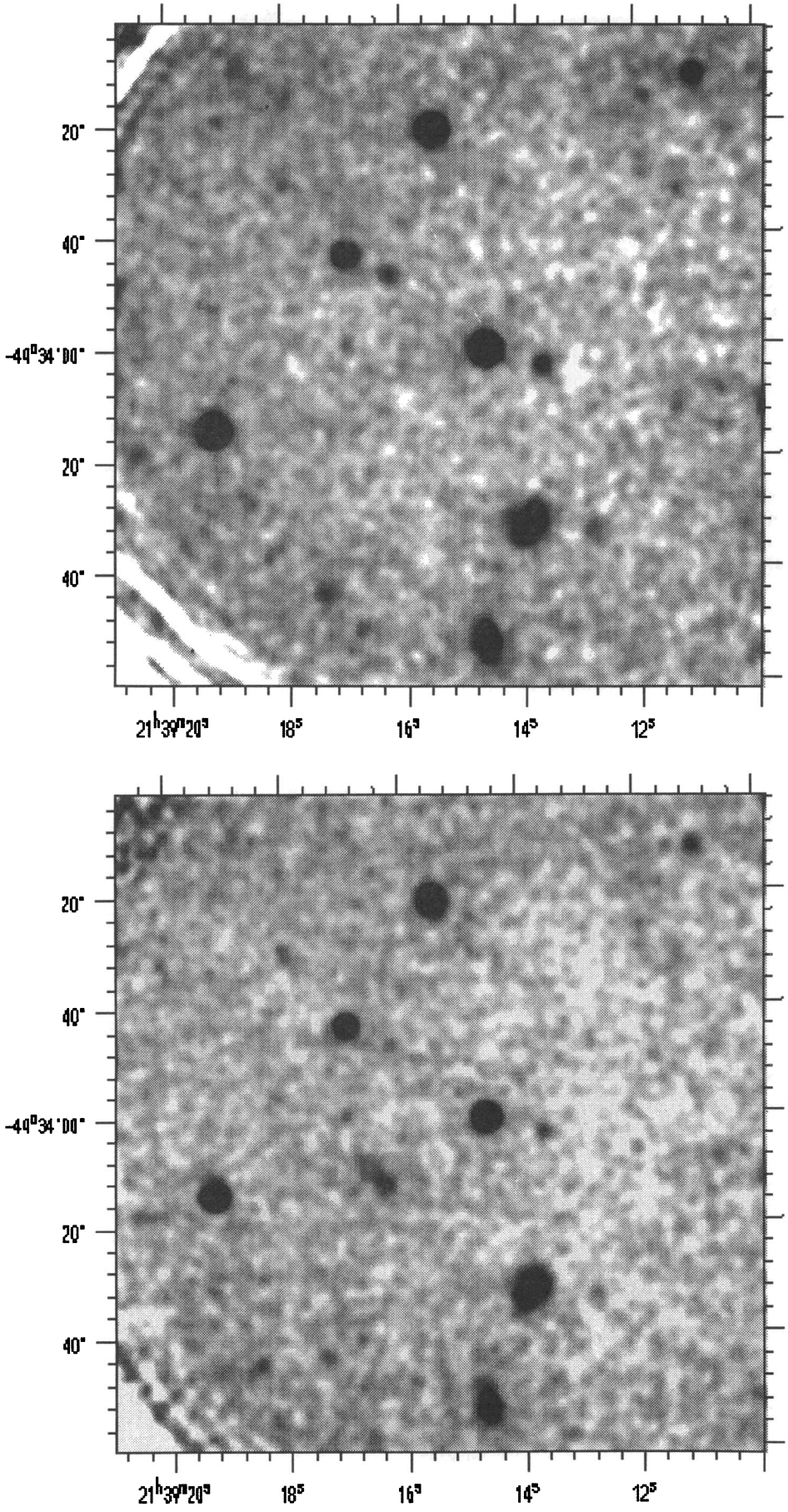

FIG. 2.—Lyα on-band (*top*) and off-band (*bottom*) images of the field around QSO 2139 − 4434. Images have been lightly smoothed by a Gaussian of $\sigma = 0\farcs6$, axes are in B1950 coordinates. See Fig. 3 for the names of the objects.

central wavelength 2.238 μm and width (FWHM) 0.048 μm, roughly matching the expected wavelength of Hα emission at $z = 2.38$. The K' image was used as the off-band image for this Hα image, and a (3 σ) flux limit of 4.5×10^{-16} ergs cm^{-2} s^{-1} was reached. Conditions were photometric, accuracy being limited by a slight time dependence in the flat field to $\sim$0.1 mag.

Further IR imaging was obtained with the IRAC-2B camera on the ESO/MPI 2.2 m telescope. Twenty-two exposures of 300 s each were taken, centered on the QSO in the J-band, in nonphotometric conditions, on 1994 October 25. Photometric calibration was obtained from five exposures of 180 s each taken on 1994 November 18 with the same instrument. Seeing was 1".1 and the 3 σ magnitude limit is 21.77. Twenty-nine exposures of 300 s were also taken in K' in photometric conditions on 1994 October 24.

2.3. *Spectroscopy*

We detected three possible Lyα-emitting galaxies in our narrowband imaging, B1, B2, and B3 (see § 3.1). Follow-up spectroscopy of two of these candidates, B1 and B2, was obtained on the nights of 1994 August 4 and 5 with the EMMI instrument (see Dekker et al. 1991) on the ESO New Technology Telescope. The slit was placed over the background QSO at such an angle that it would also cover the candidate galaxy. In the case of B1, the slit passed through the peak narrowband emission, but 2" southwest of the IR-bright nucleus. Blue-arm spectra of both objects were taken with blue medium-dispersion mode (BLMD) with the No. 3 grism and a 2" slit, which yielded a resolution of 2.35 Å. Exposure times were 7200 s for both candidates. In addition, a red-arm spectrum of B1 was taken with red imaging and low-dispersion mode (RILD), grating No. 5, a 1".5 slit, and an exposure time of 4800 s, the resolution being $\sim$7 Å.

Additional spectra of B1 were taken with the AAT on 1994 September 6. The slit was laid along the major axis of B1 and 9000 s integration obtained. Seeing was $\sim$4", which prevented us from obtaining any useful spatial information. The Royal Greenwich Observatory spectrograph, with the 600V grating set with the blaze toward the collimator, and the Faint Object Red Spectrograph were used simultaneously, with the dichroic.

2.4. *Radio Observations*

The field of all the candidate galaxies was observed with the compact array of the Australia Telescope on 1995 January 26 and 28. A total of 20 hr of observations were obtained both at 1344 and 2378 MHz, with the 6A configuration. The data were reduced with the standard procedures embodied in the MIRIAD package and CLEANed with a restoring beam of 6".8 × 4".7 at 1344 MHz and 3".8 × 2".5 at 2378 MHz. This field has also been surveyed at 847 MHz with the Molonglo Synthesis Telescope (R. W. Hunstead 1994, private communication).

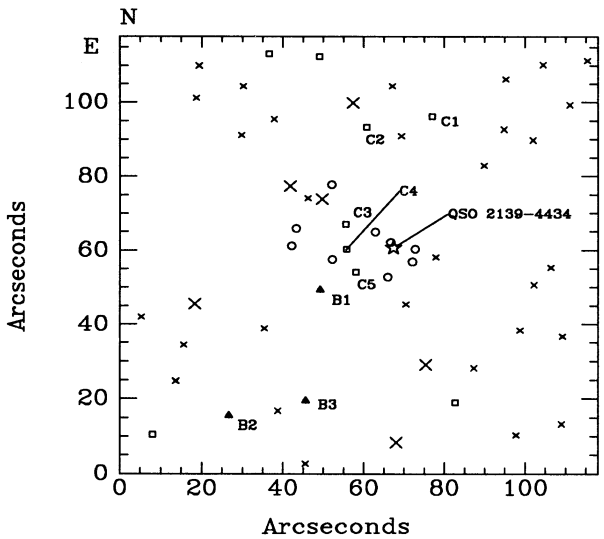

FIG. 3.—Identification chart for the images. The orientation and field of view of this chart are the same as that of Figs. 2 and 6. Triangles are Lyα-emission candidates, squares are objects with large $I - K'$ colors, i.e., candidate cluster members (§ 3.2). Circles are objects red in $B - K'$ but not in $I - K'$, i.e., candidate foreground galaxies. Other objects are marked with crosses and are probably foreground stars and galaxies.

Although radio-quiet, QSO 2139−4434 is detected at all three frequencies, with fluxes of 3.8 ± 1.1 mJy at 847 MHz, 1.61 ± 0.09 mJy at 1344 MHz, and 0.86 ± 0.09 mJy at 2378 MHz. Nothing else is detected in the field at any wavelength, 3 σ limits being 3.3 mJy (847 MHz) and 0.27 mJy (1344 and 2378 MHz).

3. RESULTS

3.1. *Line-emitting Galaxies*

We detected three candidate Lyα-emitting galaxies, B1, B2, and B3 (Figs. 2 and 3). All three were seen in the narrowband Lyα image but not in the off-band Fabry-Perot image, though B3 was detected only with $\sim$2.7 σ confidence. Our spectra of B1 and B2 show that the narrowband-image flux is indeed due to a strong, isolated emission line. For B1 we also detect C IV and Hα emission, which confirms the identification of the line as Lyα. The properties of these candidates are shown in Table 1.

Object B1 lies 22" from the background QSO and has an extended emission-line morphology (Fig. 4). A knot of Lyα flux lies to the southwest of B1, marginally resolved (FWHM $\sim$ 4", 18 kpc) and contributing roughly half the flux. The remainder comes from a tail that extends $\sim$10" (50 kpc) to the northeast.

Object B1 has an Hα flux of $(9.2 \pm 1.5) \times 10^{-16}$ ergs cm^{-2} s^{-1} (1 σ errors). The Hα emission's morphology is similar to

TABLE 1

PROPERTIES OF CANDIDATE Lyα GALAXIES

CANDIDATE	COORDINATES (B1950) R.A.	decl.	Lyα FLUX (ergs cm^{-2} s^{-1})	Lyα EQUIVALENT WIDTH (3 σ Å, observed frame)
B1	21^{h}39^{m}16^s.32	44°34'12".9	$8 \pm 1 \times 10^{-16}$	>270
B2	21 39 18.50	44 34 44.9	$3 \pm 0.3 \times 10^{-16}$	>160
B3	21 39 16.82	44 34 40.7	$0.8 \pm 0.3 \times 10^{-16}$	...
2139−4434.....	21 39 14.62	44 34 00.5	...	...

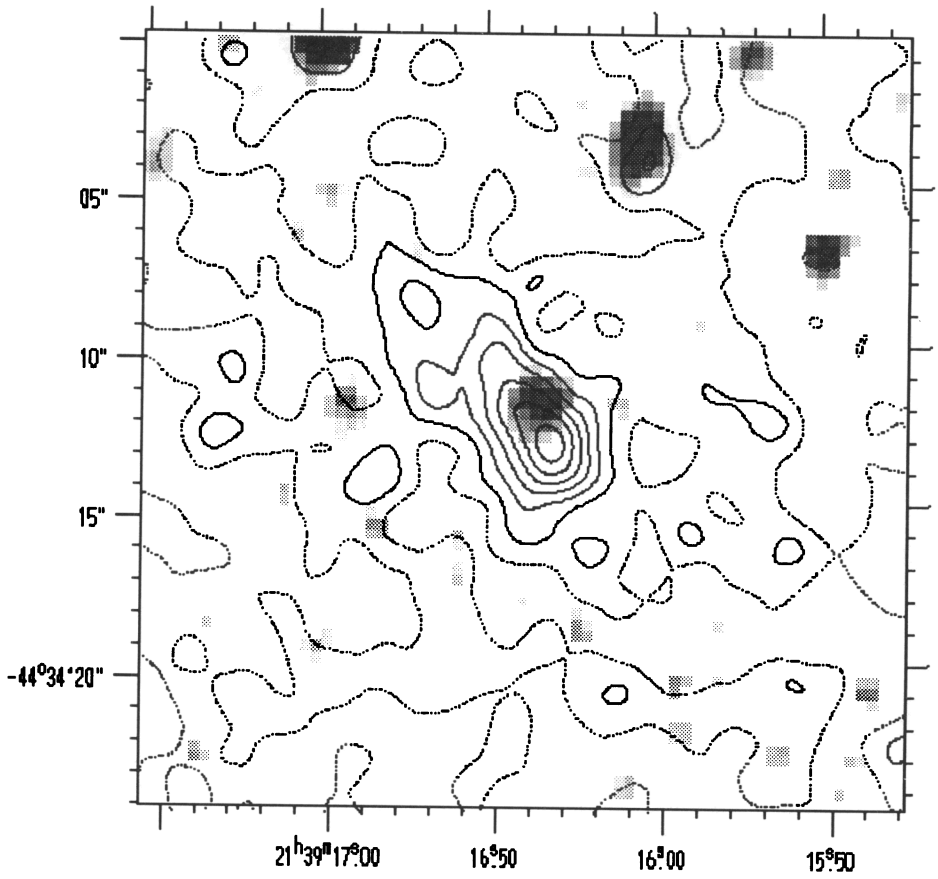

FIG. 4.—Close-up of B1. The K' image is shown in grayscale and the narrowband Lyα image (smoothed with a Gaussian beam of $\sigma = 0''.56$) is shown by contours. Contours are equally spaced; the zero-level contour is dotted. The internal astrometry of the K' and Lyα images is good to $\sim 0''.15$, based on the rms fit of the positions of all the images; the misalignment of the object in the top right is also real.

that of the Lyα morphology. Note that Hα contributes less than 10% of the K'-band flux. C IV is detected with 3 σ confidence, at a position on the slit that corresponds to the peak of the Lyα emission. The ratio of Lyα to C IV is $\sim 7:1$ at this position. A possible He II line is seen at ~ 2 σ confidence, $\sim 50\%$ weaker than C IV; no other significant emission features are seen.

The redshift of B1, as deduced from the C IV emission (Fig. 5), is 2.3796, identical within the errors (~ 100 km s^{-1}) to that of the centroid of the QSO absorption line (Fig. 5). However, the Lyα emission is redshifted by ~ 490 km s^{-1} with respect to both of these lines. The Lyα line is strongly red-asymmetric and has a velocity width of ~ 600 km s^{-1}. The apparent relative displacement of Lyα and C IV may be caused by Lyα absorption (see § 4.2).

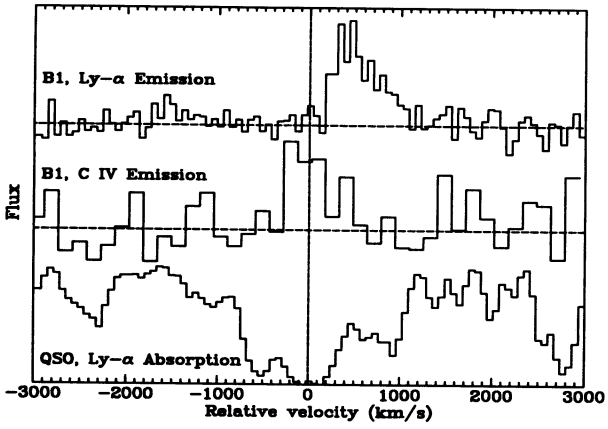

FIG. 5.—C IV and Lyα emission from B1 (NTT spectra). The Lyα absorption line in the spectrum of QSO 2139−4434 is shown for comparison.

B1 is not seen in any of the broadband optical images. No continuum is seen in the blue spectra, though a faint continuum is seen with about 2 σ confidence in the red spectrum, which yields B1 a tentative continuum magnitude of 25.8 at 5000 Å. In the near-IR, though, a strong, unresolved source is seen, which lies within the extended Lyα morphology. This source is marginally detected in the J band ($J \sim 22.0$ mag) but is relatively bright in H and K' ($H = 19.9$ mag, $K' = 19.0$ mag).

The Lyα knot and the IR source are misaligned by $\sim 2''.5$. This misalignment is real; the two images have internal astrometry accurate to $\sim 0''.15$. The colors of the IR source show a pronounced break at ~ 1.3 μm, which is the expected position of the Balmer or 4000 Å break at $z = 2.38$. Objects that show such a near-IR spectral break are rare—only four are seen in our 7800 arcsec^2 field of view. Given this surface density, the probability of such an object's lying within $2''.5$ of the peak of the Lyα emission is 0.2%. We therefore consider it highly probable that the IR source is at the same redshift as, and associated with, the Lyα emission. Hα emission comes from the same region as Lyα emission; the Hα emission is detected from both the Lyα knot and tail with greater than 4 σ confidence, with approximately equal Hα fluxes. The Hα image

also shows flux at the position of the continuum IR source, no more than would be expected from a featureless continuum spectrum. The signal-to-noise ratio of the Hα image is too poor to allow any other morphological information to be extracted.

Object B2 lies 63″ from the background QSO and is unresolved. It is marginally detected (~2 σ confidence) in the K' image ($K' \sim 20.8$ mag) and not detected in any other band. We only detected the one line in B2, but its equivalent width is much greater than that of [O II] in a typical field galaxy (Colless et al. 1990; Glazebrook et al. 1995), which strongly suggests that the line is indeed Lyα at $z = 2.38$. Hα is not detected, the upper limit being 4.5×10^{-16} ergs cm^{-2} s^{-1} (3 σ). B2's Lyα emission is redshifted by 160 km s^{-1} with respect to the absorption-line centroid and has a red-asymmetric profile and a velocity width (FWHM) of ~450 km s^{-1}. No other lines are seen in the blue spectrum, the upper limit on their flux being 30% that of Lyα, but the spectrum only covers the rest-frame wavelength region 1182–1320 Å, so no other strong lines would be expected.

B3 is detected with only ~2.7 σ confidence; we have no color or spectral information on it.

3.2. *Broadband Colors*

When we obtained IR images of our field, we were surprised to find that the QSO 2139−4434 and B1 are surrounded by a group of very red ($B - K' > 5$ mag) objects that extends over ~50″ (Fig. 6). Multicolor photometry provides some clues to the redshifts of these objects.

B1 itself, as discussed above, shows a clear spectral break at about 1.3 μm (Fig. 7), which we ascribe to the redshifted Balmer or 4000 Å break, that gives it an $I - H$ color of 3.1 mag. Most of the other red objects near it have $I - H < 2.5$ mag; they have relatively flat spectral energy distributions between the I and K' bands and very red $B - I$ colors. Spectral energy distributions of the two brightest of these objects are shown in Figure 7 as examples. These objects are unlikely to be associated with the Francis & Hewett supercluster; instead, their colors are typical of galaxies at $0.3 < z < 1.2$.

A few of B1's red neighbors do have colors consistent with a redshifted Balmer or 4000 Å break at $z \sim 2.38$. These candidate supercluster members are marked as squares in Figure 3, and their spectral energy distributions are shown in Figure 7. In most cases, they are too faint to say with confidence whether they show a strong redshifted spectral break; further deep I-band photometry will resolve this question.

A number of other objects in the field of view but more distant from B1 also have large $I - K'$ colors and, hence, are candidate $z = 2.38$ objects. These objects are also marked as squares in Figure 3, and the spectral energy distributions of the two best candidates are shown in Figure 7.

Could any of these very red objects be M dwarfs? Leggett (1992) showed that the optical/near-IR colors of M dwarfs lie in a well-defined subset of the color space. B1 and the other candidate $z = 2.38$ galaxies, however, show very different colors. In particular, their $J - K'$ colors are much redder than those of any of the dwarf stars studied by Leggett. We therefore consider it unlikely that these objects are Galactic stars.

In conclusion, the very red objects that surround the QSO and B1 fall into two classes: objects with spectral breaks between the B and I bands, which are probably foreground galaxies, and objects with spectral breaks between the I and H bands, which are probably at the same redshift as the QSO absorption lines and as B1 and B2.

3.3. *The QSO Sight Line*

The line of sight to the background QSO, 2139−4434, lies 22″ from B1. We performed a PSF subtraction on our images to look for a possible absorbing galaxy closer to the line of sight. The PSF subtraction in the Lyα and B-band images revealed nothing. The QSO is not black in the Lyα image, as our filter passband was wider than the absorption line. We would not detect objects within ~1″ of the QSO sight line.

In the I-band and the IR images, a source is seen 1.″8 from the QSO sight line, lying roughly 30° east of north. This source is most clearly seen in the K' image. This object has a flat spectral energy distribution between I and K' but is very red in $B - I$ ($B > 24$ mag, $I \sim 20.4$ mag, $K' \sim 18.3$ mag). These colors are very similar to those of the candidate foreground galaxies discussed in § 3.2, and we therefore hypothesize that, like them, this object lies at a redshift $0.3 < z < 1.2$.

Note that the presence of so many intermediate-redshift galaxies close to the QSO sight line may not be coincidental; they may be gravitationally lensing QSO 2139−4434, amplifying it enough to bring it into the QSO sample (see, e.g., Webster et al. 1988; Rodrigues-Williams & Hogan 1994).

4. DISCUSSION

4.1. *The Supercluster?*

Francis & Hewett (1993) claimed that their absorption-line supercluster has an overdensity of more than 30 (95% confidence), although they were unable to determine whether it was some sort of primordial pancake or a Great Wall–style supercluster. Our detection of galaxies near one of the QSO absorption-line clouds suggests that it is indeed a galaxy cluster and not a primordial pancake, though it may be a very gas rich supercluster. Following the argument of Wolfe (1993), we can estimate the overdensity of Lyα-emitting galaxies in the imaged field by comparing our galaxy detections with the null results reported by field searches for Lyα emission.

As our control sample, we use the search for field Lyα-emitting galaxies carried out by Pritchet & Hartwick (1990). They claimed to have searched a comoving volume 100 times larger than ours, down to a limiting flux of 5.4×10^{-17} ergs cm^{-2} s^{-1} arcsec^{-2} (2 σ). B1 has a peak surface brightness of 1.6×10^{-16} ergs cm^{-2} s^{-1} arcsec^{-2}. B2 is unresolved in ~1.″6 seeing; we measured a peak surface brightness of 9.6×10^{-17} ergs cm^{-2} s^{-1} arcsec^{-2}. Both B1 and B2 thus easily exceed their quoted flux limits unless their seeing was very poor. Pritchet & Hartwick did not explicitly state their equivalent-width limit, but they implied that their search was sensitive to objects that showed greater than 0.1 mag differences between their on- and off-band images, which implies an equivalent-width limit ≪50 Å. Both B1 and B2 have equivalent widths much greater than this. It is therefore probable that if any objects such as B1 and B2 existed in the region surveyed by Pritchet & Hartwick they would have been found.

We calculate limits on the overdensity of Lyα galaxies in our field as follows: First, we assume a background Lyα-galaxy density ρ and an overdensity ω of Lyα galaxies in our field, defined as the ratio of the mean Lyα-galaxy density in our field divided by the background Lyα-galaxy density. Using Poisson statistics, we then derive the probability of seeing two or more galaxies in our field, P_f, and the probability of seeing no galaxies in Pritchet & Hartwick's survey, P_p. We then vary ρ to maximize the joint probability $P_j = P_f P_p$ for a given value of ω.

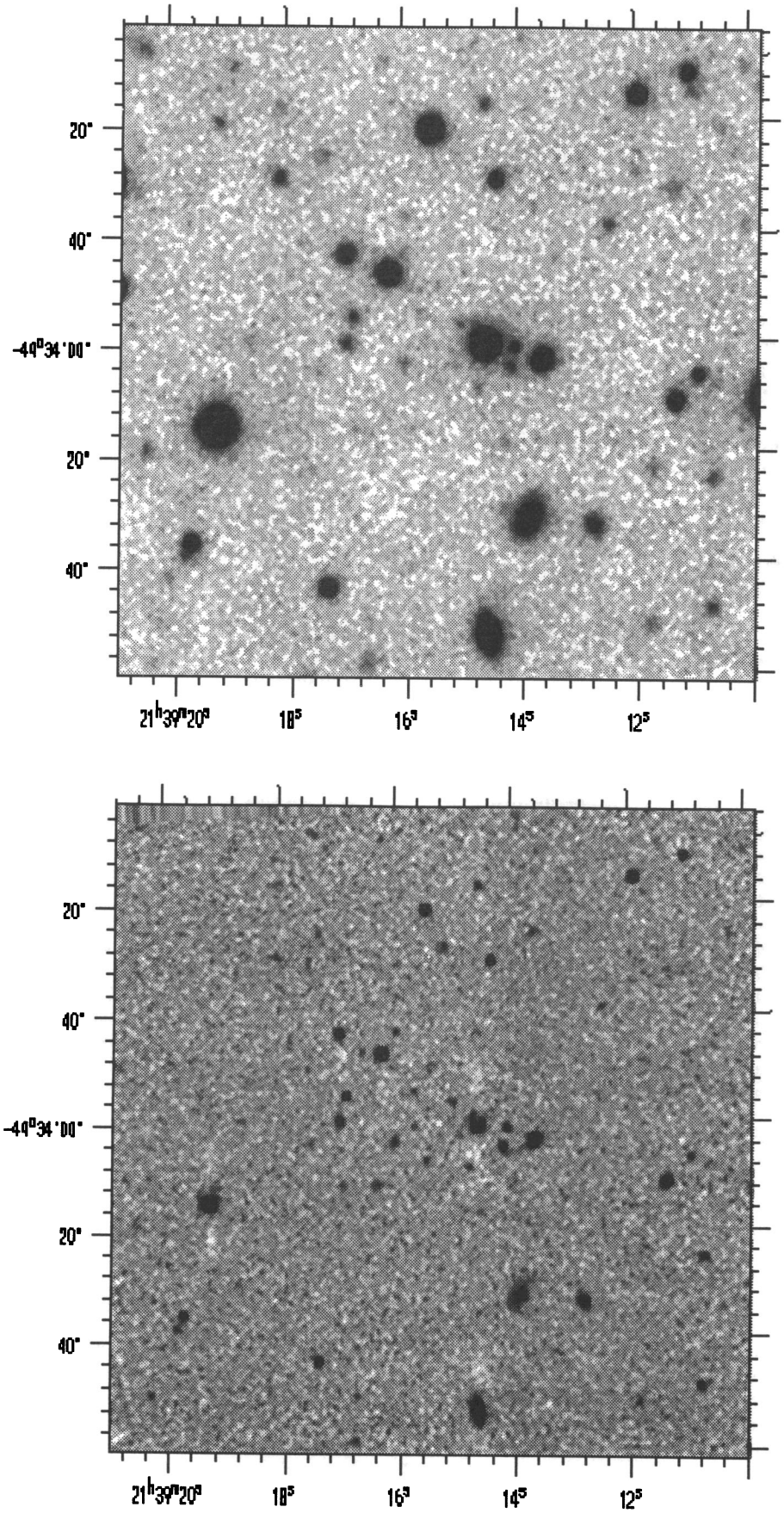

FIG. 6.—*I*-band (*top*) and Siding Spring 2.3 m *K'*-band (*bottom*) images. The white patches above and below the brightest sources are artifacts of the data reduction.

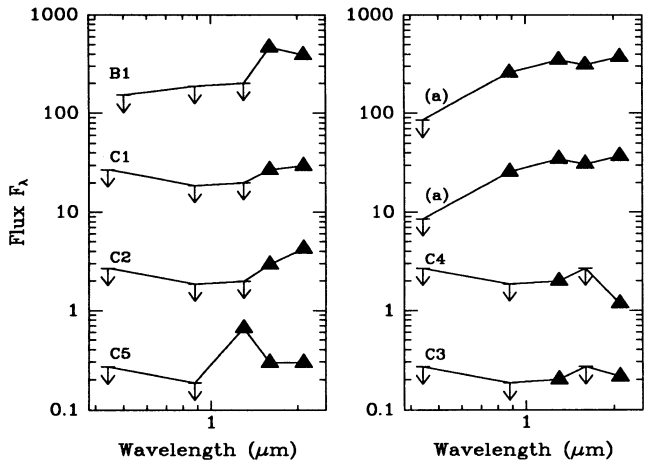

FIG. 7.—Spectral energy distributions for a number of candidate galaxies. The distributions marked "(a)" are for two representative red objects that show a break between B and I, i.e., candidate foreground galaxies. The different objects have displaced vertical scales for clarity. The data points are for standard B, I, J, H, and K' bands except for B1, where a more stringent limit on the blue flux is placed at 5000 Å from our spectra.

If our field is in no way special ($\omega = 1$), the peak joint probability is 5×10^{-5}. We can therefore reject the null hypothesis that Lyα galaxies are not overdense in our field. For larger values of ω, the maximum joint probability increases and occurs for smaller ρ. To bring P_j up to 5%, we require that $\omega > 15$; our field must have an overdensity of a factor of at least 15 (95% confidence).

An overdensity of more than 15 in our 2′ radius field, while consistent with Francis & Hewett's claim, is not in itself very surprising; 2′ corresponds to a proper-distance scale of $\sim$500 kpc, and overdensities greater than 15 on these scales are common in the Local universe. If, however, the overdensity remains this high over the whole postulated supercluster, greater than 8′ in diameter, this would be surprising. The only object in the Local universe that approaches such overdensities on these large scales is the Great Wall. Heisler et al. (1989) and Wolfe (1993) argued that the existence of structures this large and dense at high redshifts is a challenge for gravitational-structure formation models such as CDM. The location of B2, C1, and C2 near the edge of our field of view suggests that the overdensity of galaxies does indeed continue beyond the field we have imaged to date.

The main weakness with this analysis is the control sample. Pritchet & Hartwick's sample is at the slightly lower redshift $z \sim 1.9$. If the number density of Lyα galaxies was evolving strongly between $z = 2.38$ and $z \sim 1.9$, the overdensity in our field might be much lower. De Propris et al. (1993) carried out a field search for Lyα-emitting galaxies between redshifts 2 and 3 and discovered none, but unfortunately their survey was insufficiently deep to detect objects with fluxes comparable to B1 and B2. The many other unsuccessful Lyα-galaxy searches, many at redshifts above 2.38 (e.g., Lowenthal et al. 1995; Djorgovski, Thompspn, & Smith 1993), make us doubt that the numbers of Lyα galaxies are evolving strongly. It is also worrisome that Pritchet & Hartwick selected their candidates by eye; De Propris et al. (1993), using an almost identical technique, only found $\sim$50% of simulated 10 σ galaxies. Clearly, a quantitative analysis of deeper control fields at $z \sim 2.4$ would help.

If one assumes that our analysis is valid and that the overdensity of galaxies really does extend to megaparsec scales, one possible explanation is that the distribution of Lyα-emitting galaxies is strongly decoupled from that of the underlying matter. If, for example, Lyα-emitting galaxies only form at very high density peaks in the underlying mass distribution, they will be far more strongly clustered than matter (see, e.g., Kaiser 1984). Brainerd & Villumsen (1994) showed that in n-body CDM simulations dark matter halos cluster far more strongly than the underlying mass at $z \sim 2$. Evidence for such biasing comes from the very different clustering amplitudes inferred for Lyα forest clouds and metal-line QSO absorption systems (Carswell & Rees 1987; Heisler et al. 1989).

4.2. *The Nature of B1*

In recent years, a small number of Lyα-emitting galaxies have been found near QSO absorption-line systems (see Lowenthal et al. 1991; Møller & Warren 1993; Machetto et al. 1993; Steidel, Sargent, & Dickinson 1991). Most are very compact and, at best, marginally resolved, unlike B1.

The morphology of B1 is, however, typical of high-redshift radio galaxies, which form the vast majority of known high-redshift galaxies (McCarthy 1993). B1 resembles these galaxies in many ways: in its elongated, irregular morphology, its Lyα flux and equivalent width, its line ratios, its red continuum colors, and its red companion objects (Rigler et al. 1992). It lies on the K-band Hubble diagram for powerful radio galaxies. There are, though, two significant differences—B1's radio flux is at least 2 orders of magnitude below that of radio galaxies with comparable emission-line fluxes, and the velocity width of Lyα is about half that of a typical radio galaxy (though this may be due to absorption). Nonetheless, the similarity between B1 and many radio galaxies is striking.

B1 consists of an IR-bright, unresolved core (rest-frame absolute V-band magnitude of approximately -24.4 mag) and an extended, asymmetric, line-emitting tail (Fig. 4). As shown in § 3.2, the core has a pronounced spectral break at $\sim$1.3 μm observed-frame, which gives it a rest-frame color of $U - V > 1$ mag. Our narrowband Hα imaging shows that only less than 10% of the K' flux comes from line emission, so we attempted to fit B1's colors using synthetic galaxy spectra from Arimoto & Yoshii (1987), Arimoto, Yoshii, & Takahara (1992), Bruzual & Charlot (1993), and Rocca-Volmerange & Guiderdoni (1988). The magnitude of the spectral break can only be reproduced by stellar populations with little ongoing or recent star formation; a population of stars formed in an instantaneous burst and then allowed to passively age for more than 0.6 Gyr gives a good fit. If the age is $\sim$0.6 Gyr, the 1.3 μm break would be due to Balmer absorption in A stars, whose light is expected to dominate galaxies of this age. If older, the break would be the well-known 4000 Å feature. The stellar mass M derived from the rest-frame V-band light is somewhat model dependent, being somewhere in the range $\sim 2 \times 10^{11}\ M_\odot < M < \sim 2 \times 10^{12}\ M_\odot$. Models in which star formation is ongoing or recent predict 0.5 μm fluxes significantly above our limits, due to a population of O and B stars. If the tentative detection of continuum flux at 5000 Å in the red spectrum were correct, a small number of blue stars or some nonthermal component would be required. An age of $\sim$0.5 Gyr at $z = 2.38$ implies (for $H_0 = 75$ km s^{-1} Mpc^{-1}) that formation occurred at $z \sim 3.7$ ($q_0 = 0.5$) or $z \sim 3.0$ ($q_0 = 0.1$). If the age were 1 Gyr, the epoch of formation would be $z \sim 5$ ($q_0 = 0.5$) or $z \sim 4$ ($q_0 = 0.1$).

What is the cause of the line emission? The Lyα and Hα flux could be generated by star formation at a rate of $\sim 100\ M_\odot$

yr^{-1} (Kennicutt 1983) without overproducing blue continuum light (Charlot & Fall 1993). However, the detection of C IV strongly suggests that an active galactic nucleus (AGN) is present, as hot stars produce few photons capable of ionizing carbon to this state. The similarity between B1 and radio galaxies also suggests that an AGN is present, albeit a radio-quiet one.

The Lyα equivalent width of B1 is higher, and the Lyα line narrower, than those of typical QSOs (Francis et al. 1992; Francis 1993). If, however, the active nucleus were hidden from direct observation by dust clouds but its radiation could escape in other directions, we would only see scattered light and line emission from photoionized gas far from the nucleus, which might have much higher equivalent widths and lower velocity widths. This is now known to be the explanation of strong narrow lines of many Seyfert 2 galaxies (see, e.g., Antonucci & Miller 1985) and is widely invoked to explain the line emission of radio galaxies.

Many high-redshift QSOs and radio galaxies show extended Lyα emission with fluxes in excess of B1's, originating on scales of up to 100 kpc (see, e.g., Heckman et al. 1991). An AGN with an absolute B magnitude of -23 mag produces enough ionizing photons to generate the observed Lyα and Hα fluxes. If the Lyα flux were produced by photoionization from an AGN concealed in the IR-bright core, the asymmetry of the emission would have to be caused by a highly asymmetric, lumpy gas distribution. Our upper limit on the radio flux of B1 is not inconsistent with the typical radio fluxes of the least radio-loud QSOs (Kellerman et al. 1989).

B1's Lyα emission peaks $\sim$490 km s^{-1} to the red of its C IV emission (Fig. 5). We suggest that this offset is caused by Lyα absorption of the blue part of the Lyα line. If the absorbing neutral hydrogen is dust-free, it cannot be physically associated with the emission-line region, as it would scatter roughly as many photons into the line of sight as out of it (unless the geometry were very special). If the absorber is indeed a foreground screen of neutral hydrogen, its redshift and column density have to be similar to those of the central component of the QSO absorption line. The Lyα emission would need to be intrinsically red-asymmetric and to have an intrinsic velocity width of $\sim$1000 km s^{-1}.

If, alternatively, the absorption occurs in neutral hydrogen mixed with the emission-line gas, dust is needed to absorb the resonantly scattered Lyα photons. The red wing of Lyα might escape because the high-velocity gas is dust-free or because the optical depth of the high-velocity gas is low.

We conclude that B1 is probably a large early-type galaxy that contains a hidden radio-quiet QSO, which is photoionizing the lumpy, surrounding gas.

4.3. *The Evidence for Dust*

The observed Lyα-to-Hα ratio of B1 is $\sim$0.8, well below the case B recombination value of 8. This strongly suggests that dust is present. The Lyα-Hα ratio is low in both the Lyα knot and the tail, so the dust must extend over at least 50 kpc.

If all the dust is in a foreground screen, an extinction $E(B-V) \sim 1$ mag is required to explain the observed ratio. Much smaller amounts of dust will suffice if it is mixed in with the gas, as the optical depth of the gas to resonant scattering of Lyα is likely to be large, giving the Lyα photons many chances to be absorbed.

The presence of extended dust in B1, associated with the QSO absorption-line system, supports the contention of Fall & Pei (1993) that high column density Lyα QSO absorption-line systems contain dust and, therefore, can obscure background QSOs. Given the steepness of the QSO luminosity function, even very small quantities of dust in absorption-line systems will seriously bias absorption-line statistics and QSO number counts (see, e.g., Webster et al. 1995).

4.4. *The Environment of B1*

The region around B1 and the QSO is an extraordinary one. Within a radius of $\sim$10″, we have three Lyα absorption components, one Lyα-emitting galaxy, and possibly three less active galaxies, C3, C4, and C5. If they are physically associated, they all lie within $\sim$100 kpc of each other.

If C3, C4, and C5 really are inactive galaxies at $z = 2.38$, then, together with B1, they form a high-redshift analog of a compact group (Hickson, Kindl, & Huchra 1989). Many more galaxies could be present but below our detection threshold. The extended, irregular emission of B1 suggests that this group of galaxies is embedded in a lumpy cloud of dust and gas.

The absorption in the spectrum of QSO 2139$-$4434 also suggests the presence of a lumpy gas cloud. It is interesting that the column density of the main QSO absorption component is similar to that needed to absorb the blue wing of B1's Lyα emission (§ 4.3). If the QSO absorption components really are associated with the gas cloud in which B1, C3, C4, and C5 are embedded, we can estimate the mass of this gas cloud: a gas cloud of column density $N_{\rm H} \sim 10^{19}$ cm^{-2} and radius 50 kpc will have a neutral hydrogen mass of $\sim 2 \times 10^9\ M_\odot$, i.e., $\sim$5% of the stellar mass of B1.

On a yet more speculative note, if all three absorption-line components are associated with the galaxy group, we can combine their redshifts with that of B1 to estimate a velocity dispersion for the gas cloud of $\sim$500 km s^{-1}. This calculation should be regarded with great caution; quite apart from the small number statistics, the velocities of the three absorption-line components could be dominated by the gravity of a compact galaxy hidden in the PSF of the QSO. Alternatively, they may lie in different parts of Francis & Hewett's (1993) supercluster; if the absorption-line supercluster is roughly spherical and expanding with the Hubble flow, it will have an expected radial extent of $\sim$1000 km s^{-1}, greater than the velocity differences between the different absorption-line components. If, however, 500 km s^{-1} is a reasonable estimate of the velocity dispersion of the group and this velocity dispersion is dominated by gravitational motions and not by gas dynamics, the virial mass of the group is $\sim 10^{12}\ M_\odot$ and the crossing time is $\sim 10^8$ yr.

Irrespective of the velocity dispersion of the group, if B1 and its neighbors are gravitationally bound, their merger timescale will be $\ll$1 Gyr (but see Governato, Bhatia, & Chincarini 1991). We therefore speculate that, by redshift zero, B1 will have accreted C3, C4, C5, and much of its gaseous halo to form a massive elliptical galaxy, perhaps even a cD galaxy.

To summarize, if B1, the color-selected galaxies, and the QSO absorption-line clouds really are physically associated, they form an extremely gas-rich compact group, which may be a giant elliptical galaxy in the process of bottom-up formation.

5. CONCLUSION

We have detected and confirmed two Lyα-emitting galaxies at $z = 2.38$, associated with a cluster of Lyα QSO absorption lines. One of these galaxies, B1, lies 22″ from a background QSO and is surrounded by a group of very red objects, some of

which may be other galaxies at the same redshift. The detection of two Lyα-emitting galaxies in the small area surveyed supports Francis & Hewett's (1993) claimed supercluster, though final proof will require the mapping of the rest of the postulated supercluster.

B1 is a massive early-type galaxy, at least 500 Myr old, and probably contains a concealed radio-quiet AGN, which is photoionizing an irregular cloud of gas that surrounds B1. Together with its neighboring red galaxies, it may be a giant elliptical galaxy in the process of bottom-up formation.

We have detected Hα emission from B1 at a level that indicates dust is present. This supports Hu et al.'s (1993) and Bunker et al.'s (1995) contention that Hα searches may be a powerful tool for finding high-redshift galaxies. The dust is extended over at least 50 kpc, which supports Fall & Pei's (1993) contention that dust obscuration is important in QSO absorption lines.

The pronounced 1.3 μm break in the spectrum of B1 suggests an additional technique for finding high-redshift galaxies. With optical and near-IR photometry, it may be possible to select galaxies by the presence of a redshifted Balmer or 4000 Å break. The technique is similar to Steidel & Hamilton's (1992) broadband selection of galaxies that show Lyman limit breaks but is sensitive to lower redshifts and older galaxies.

We wish to thank Ken Freeman, Dick Hunstead, Bruce Peterson, and Rachel Webster for helpful discussions. Dick Hunstead and Taisheng Ye kindly made their Molonglo radio observations available to us. P. J. F. is supported by an ARC grant and acknowledges travel support from ANSTO. M. M. acknowledges the support of a University of Melbourne Fellowship for Women with Career Interruptions. A. J. B. acknowledges a UK Particle Physics and Astronomy Research Council studentship. Y. Y. acknowledges financial support from the Yamada Science Foundation for transport of the PICNIC camera and IR team. Astrometry was performed with coordinates from the COSMOS database, maintained on-line by the Anglo-Australian Observatory.

REFERENCES

Arimoto, N., & Yoshii, Y. 1987, A&A, 173, 23
Arimoto, N., Yoshii, Y., & Takahara, F. 1992, A&A, 253, 21
Antonucci, R. R. J., & Miller, J. S. 1985, ApJ, 297, 621
Brainerd, T. G., & Villumsen, J. V. 1994, ApJ, 431, 477
Bruzual A., G., & Charlot, S. 1993, ApJ, 405, 538
Bunker, A. J., Warren, S. J., Hewett, P. C., & Clements, D. L. 1995, MNRAS, 273, 513
Butcher, H., & Oemler, A., Jr. 1978, ApJ, 219, 18
Carswell, R. F., & Rees, M. J. 1987, MNRAS, 224, 13P
Charlot, A., & Fall, S. M. 1993, in First Light in the Universe, ed. B. Rocca-Volmerange et al. (Gif-sur-Yvette: Ed. Frontiéres), 341
Colless, M., Ellis, R. S., Taylor, K., & Hook, R. N. 1990, MNRAS, 244, 408
De Propris, R., Pritchet, C. J., Hartwick, F. D. A., & Hickson, P. 1993, AJ, 105, 1243
Dekker, H., D'Odorico, S., Kotzlowski, K., Lizon, J.-L., Longinotti, A., Nees, W., & De Lapparent-Gurriet, V. 1991, Messenger, 63, 73
Djorgovski, S., Spinrad, H., McCarthy, P., & Strauss, M. A. 1985, ApJ, 299, L1
Djorgovski, S., Thompson, D., & Smith, J. D. 1993, in First Light in the Universe, ed. B. Rocca-Volmerange et al. (Gif-sur-Yvette: Ed. Frontiéres), 67
Dressler, A., Oemler, A., Jr., Gunn, J. E., & Butcher, H. 1993, ApJ, 404, L45
Eckert, W., Hofstadt, D., & Melnick, J. 1989, Messenger, 57, 66
Edge, A. C., Stewart, G. C., Fabian, A. C., & Arnaud, K. A. 1990, MNRAS, 245, 559
Efstathiou, G., Bernstein, G., Katz, N., Tyson, J. A., & Guhathakurta, P. 1991, ApJ, 380, L47
Fall, S. M., & Pei, Y. C. 1993, ApJ, 402, 479
Foltz, C. B., Hewett, P. C., Chaffee, F. H., & Hogan, C. J. 1993, AJ, 105, 22
Francis, P. J. 1993, ApJ, 405, 119
Francis, P. J., & Hewett, P. C. 1993, AJ, 105, 1633
Francis, P. J., Hewett, P. C., Foltz, C. B., & Chaffee, F. H. 1992, ApJ, 398, 476
Gebhardt, K., Pryor, C., Williams, T. B., & Hesser, J. E. 1994, AJ, 107, 2067
Giavalisco, M., Steidel, C. C., & Szalay, A. S. 1994, ApJ, 425, L5
Glazebrook, K., Ellis, R., Colless, M., Allington-Smith, J., & Tanvir, N. 1995, MNRAS, 273, 157
Governato, F., Bhatia, R., & Chincarini, G. 1991, ApJ, 371, L15
Heckman, T. M., Lehnert, M. D., van Breugel, W., & Miley, G. K. 1991, ApJ, 370, 78
Heisler, J., Hogan, C. J., & White, S. D. M. 1989, ApJ, 347, 52
Hickson, P., Kindl, E., & Huchra, J. P. 1988, ApJ, 331, 64
Hu, E. M., Songaila, A., Cowie, L. L., & Hodapp, K.-W. 1993, ApJ, 419, L13
Jakobsen, P., & Perryman, M. A. C. 1992, ApJ, 392, 432
Kaiser, N. 1984, ApJ, 284, L9
Kellerman, K., Sramek, R., Schmidt, M., Shaffer, D., & Green, R. 1989, AJ, 98, 1195
Kennicutt, R. C., Jr. 1983, ApJ, 272, 54
Kobayashi, Y., Fang, G., Minezaki, T., Waseda, K., & Nakamura, K. 1994, Proc. SPIE, 2198, 603
Leggett, S. K. 1992, ApJS, 82, 351
Lowenthal, J. D., Hogan, C. J., Green, R. F., Caulet, A., Woodgate, B. E., Brown, L., & Foltz, C. B. 1991, ApJ, 377, L73
Lowenthal, J. D., Hogan, C. J., Green, R. F., Woodgate, B. E., Caulet, A., Brown, L., & Bechtold, J. 1995, ApJ, 451, 484
Machetto, F., Lipari, S., Giavalisco, M., Turnshek, D. A., & Sparks, W. B. 1993, ApJ, 404, 511
McCarthy, P. J. 1993, ARA&A, 31, 639
Møller, P. 1995, A&A, in press
Møller, P., & Warren, S. J. 1993, A&A, 270, 43
Pritchet, C. J., & Hartwick, F. D. A. 1990, ApJ, 355, L11
Rigler, M. A., Lilly, S. J., Stockton, A., Hammer, F., & Le Fèvre, O. 1992, ApJ, 385, 61
Rocca-Volmerange, B., & Guiderdoni, B. 1988, A&AS, 75, 93
Rodrigues-Williams, L. L., & Hogan, C. J. 1994, AJ, 107, 451
Steidel, C. C., & Hamilton, D. 1992, AJ, 104, 941
Steidel, C. C., Sargent, W. L. W., & Dickinson, M. 1991, AJ, 101, 1187
Webster, R. L., Francis, P. J., Peterson, B. A., Drinkwater, M. J., & Masci, F. J. 1995, Nature, 375, 469
Webster, R. L., Hewett, P. C., Harding, M. E., & Wegner, G. A. 1988, Nature, 336, 358
Williger, G. M., Hazard, C., Baldwin, J. A., & McMahon, R. G. 1995, ApJ, submitted
Wolfe, A. M. 1993, ApJ, 402, 411